AMERICAN METEOROLOGICAL SOCIETY

Journal of Atmospheric and Oceanic Technology

The DOI for this manuscript is doi: 10.1175/JTECH-D-17-0141.1

A correction for the thermal mass induced-errors of CTD tags mounted on marine mammals

Vigan Mensah[1], Fabien Roquet[2,3], Lia Siegelman-Charbit[4,5], Baptiste Picard[6], Etienne Pauthenet[2], Christophe Guinet[6]

[1] Institute of Low Temperature Science, Hokkaido University, Sapporo, Japan

[2] Department of Meteorology at Stockholm University (MISU), Stockholm University, Stockholm, Sweden

[3] Department of Marine Sciences, University of Gothenburg, Goteborg, Sweden

[4] Marine Environmental Science Laboratory (LEMAR), Plouzane, France

[5] Laboratory for Ocean Physics and Remote Sensing (LOPS), Plouzane, France

[6] Centre d'Etude Biologiques de Chize (CNRS), Villiers-en-Bois, France

Correspondence to: V. Mensah, vmensah@lowtem.hokudai.ac.jp

Abstract

The effect of thermal mass on the salinity estimate from Conductivity Temperature Depth (CTD) tags sensor mounted on marine mammals is documented and a correction scheme is proposed to mitigate its impact. The algorithm developed here allows for a direct correction of the salinity data, rather than a correction of the sample's conductivity and temperature. The amplitude of the thermal mass induced error on salinity and its correction are evaluated via comparison between data from CTD tags and from Seabird Scientific © CTD used as a reference. Thermal mass error on salinity appears to be generally of order $O(10^{-2})$ $g.kg^{-1}$, may reach $O(10^{-1})$ $g.kg^{-1}$, and tends to increase together with the magnitude of the cumulated temperature gradient (T_{HP}) within the water column. The correction we propose yields an error decrease of up to ~ 60% if correction coefficients specific to a certain tag or environment are calculated, and up to 50% if a default value for the coefficients is provided. The correction with the default coefficients was also evaluated using over 22000 in-situ dives data from 5 tags deployed in the Southern Ocean and is found to yield significant and systematic improvements on the salinity data including for profiles whose T_{HP} was weak and the error small. The correction proposed here yields substantial improvements in the density estimates although a thermal-mass induced error in temperature measurements exists for very large T_{HP} and has yet to be corrected.

1. Introduction

The Conductivity-Temperature-Depth Satellite Relay Data Loggers (CTD-SRDL) tags (referred as "tag" in the following), developed at the Sea Mammal Research Unit (SMRU, St Andrews, UK) are routinely deployed on various species of seals, such as Southern elephant seals *Mirounga leonina,* Steller sea lions *Eumetopias jubatus*, or Ribbon seals *Histriophoca fasciat*. They represent a tremendous source of hydrographic data in largely under-sampled areas as the Southern Ocean or the northern subpolar regions (Roquet et al. 2014, Treasure et al. 2017, see meop.net for more information). The temperature and conductivity sensors fitted on tags, manufactured by Valeport Ltd. (Totnes, UK), yield high precision ($\pm$0.005 for temperature and $\pm$0.01 $ms.cm^{-1}$ for conductivity, see Boehme et al. 2009) and reasonable accuracies ($\pm$0.02 °C for temperature and $\pm$0.03 psu for salinity) after delayed-mode calibration (Roquet et al., 2011). However, a recent study by Nakanowatari et al. (2017) demonstrated that the tags are also affected by a thermal mass error -a phenomenon due to the transfer of heat from the sensor's walls to the sample being measured- on both their temperature and conductivity cells. Salinity being estimated via measurements of conductivity and temperature, the error in these measurements reflects on the salinity estimates, which display large discrepancies across sharp thermoclines.

The thermal mass phenomenon and its effect on salinity data have been well documented for the Seabird Scientific © SBE4 conductivity sensor (Lueck, 1990) and manifests in areas of large temperature gradients, such as the seasonal thermocline, where large salinity spikes of $O(10^{-2})$ psu to $O(10^{-1})$ psu appear, followed by a slow decaying hysteresis. A correction model has been developed by Lueck and Picklo (1990), and adjustments to the correction coefficients have subsequently been implemented by Morison et al. (1994), Mensah et al. (2009), Garau et al.

(2011) and Liu et al. (2015). Nakanowatari et al. (2017) successfully applied the correction method on a set of 8 tags deployed on seals in the Okhotsk Sea between 2011 and 2014, proposing a set of correction coefficients validated by comparing corrected salinity results with spatially and temporally averaged historical data. However, the effectiveness of this correction methodology in various oceanic conditions and geographical locations merits to be further assessed.

In this paper, we first document the effects of thermal mass error on the tags data by comparing results of temperature, conductivity and salinity profiles obtained simultaneously by tags and by SBE CTDs attached together on the same frame. We then develop and implement a thermal mass correction model loosely based on Lueck and Picklo (1990) -but applied directly on the salinity data- and we estimate its effectiveness on our comparison dataset. The data tested for this study having been sampled under various hydrographic and thermocline conditions, we can therefore correct each tags data with two different sets of correction coefficients: (1) a set of coefficients optimized for each specific tag sensor, and (2) a unique set of coefficients (thereafter called generic coefficients) valid for any tag sensors and in any oceanic conditions. The current study builds on Nakanowatari et al. (2017), proposing a comprehensive assessment of the effects of thermal mass error on CTD-SRDL tag measurements and aims at proposing a generic method to optimally reduce thermal mass induced-errors.

The thermal mass error affecting the tags and the salinity correction method are introduced in section 2. Section 3 presents the implementation of the correction scheme, the comparison of corrected tags data vs. reference CTD data, as well as a discussion on the effect of the correction obtained with the optimized and generic sets of correction coefficients. The generic coefficients are further tested on tens of thousands of in-situ profiles in the Southern

Ocean using upcast and downcast data as a mean of comparison, and these results are presented in section 4. A summary and conclusion are proposed in section 5.

2. Thermal mass induced-errors and its correction for CTD and tags sensors.

2.1. Theory

The thermal mass is a well-known phenomenon which affects primarily the conductivity cells of various CTD sensors, especially when the cell is unpumped as is the case for the tags. Inductive conductivity cells are made of a cylinder through which the water flows as the CTD conducts its profile. Depending on the constructor, the cell is made of glass or ceramic and is typically surrounded by a layer of epoxy for protection. During profiling, the heat capacity of the sensor's walls and protective layer causes heat to be stored within the sensor. This heat or "thermal mass" is exchanged through the sensor's walls, thus contaminating the temperature - and hence the conductivity- of the water sample. While the temperature is accurately measured by the separate CTD temperature sensor, the sample's conductivity is modified due to the thermal mass, which yields a significant discrepancy in the salinity estimation. This error has been observed on the Seabird Scientific © SBE4 conductivity cell -which is part of the SBE9 CTD system- and depends on the temperature gradient (function of depth or time). It is particularly evident in situations of sharp thermocline (Lueck and Picklo, 1990; Morison et al., 1994; Mensah et al., 2009; Liu et al., 2015). This issue has been addressed in several works, with a thermal correction model developed by Lueck (1990) specifically for the SBE sensor. In that study, the thermal mass error is modelled as an error amplitude α_C, decaying within a relaxation time $1/\beta$ (Lueck, 1990). The conductivity is then corrected via

$$C_T(n) = \Gamma_C \alpha_C (1 - 0.5\beta\Delta_t)^{-1} T_{HP}(n), \quad (1),$$

where C_T is the correction of conductivity added to the conductivity of the nth sample, $T_{HP}(n)$ is the high-pass filtered sample's temperature (see Eq. (A4) Appendix I), using a first-order discrete-time filter with a time constant $\tau = \beta^{-1} - 0.5\Delta_t$, n is the sample index, $\Gamma_C = \frac{\partial C}{\partial T_{S,p}}$ is the coefficient of sensitivity of conductivity to temperature, and Δ_t is the sampling time interval. This model has been successfully implemented with various sets of α_C and β coefficients for the SBE4. In the limit case $\Delta_t\beta \ll 1$ (i.e. when the response time is much larger than the sampling interval), the correction simply becomes $C_T = \Gamma_C \alpha_C T_{HP}$ with a time constant = β^{-1}. Note that the formulation of the correction given here differs from the one given in Lueck and Picklo (1990), however both are formally equivalent as shown in Appendix I. The formulation given here is preferred because it is more readily interpretable in terms of a standard discrete-time high-pass filter.

The setting and technology of the tag sensor differ from those of the SBE4 cell, in that the wall of the conductivity sensor is made of ceramic for the tag instead of glass for the CTD cell, and the latter is an electrode cell whereas the tag cell is inductive. Despite these design differences, the tags are likely to show similar signs of thermal mass-induced anomalies due to the water sample passing through a few centimeters long pipe, itself covered by epoxy resin. The thickness of the epoxy layer is sensibly larger than on the SBE4 cell and, should the tag sensor indeed be affected by a thermal mass error, longer relaxation time than for the SBE cell are expected. Importantly, the Platinum Resistance Temperature sensor being located in the immediate vicinity upstream of the conductivity cell and surrounded by epoxy, a thermal mass error may also affect the temperature measurements, contrary to the SBE CTD.

Following Morison et al. (1994), temperature could be corrected with a similar scheme as conductivity according to

$$T_T(n) = \alpha_T(1 - 0.5\beta\Delta_t)^{-1}T_{HP}(n) \quad (2),$$

where the only formal difference with (1) is that no sensitivity coefficient is required in the case of a temperature correction.

2.2. Illustration of the thermal mass error on tags data

In order to assess the possibility of a thermal mass error affecting both the tags temperature and conductivity sensors, we tested the response of four tags to high temperature gradients in *in-situ* situations. As part of the "BOUSSOLE" program (Antoine et al., 2006; Antoine et al., 2008) in the Ligurian Sea, the four sensors were attached together with a SBE9 CTD system, which is used as a reference, and 7 casts were conducted. Each tag temperature, conductivity and salinity profiles are corrected for bias and pressure-induced slope following Roquet et al. (2011). The test was conducted at the BOUSSOLE mooring site (43°20'N, 7°54'E) in the northwestern Mediterranean sea, on board the SSV "Tethys II". The experiment was carried out on the 11th and 12th of June 2008, during which a seasonal thermocline of gradient ~0.2 °C.m^{-1} occurred between ~10 m and ~50 m depth, and with local maximum gradient of ~0.6 °C.m^{-1}. Our test is therefore suited for detecting and characterizing errors in a nearly idealized, step-like environment, as it was done in Lueck and Picklo (1990), Morison et al. (1994) or Mensah et al. (2009). The results of this experiment are illustrated in Figure 1, where profiles of temperature, conductivity and salinity (Figure 1a-c) are plotted for both CTD and tags, whereas the difference between the sensors are plotted in Figures 1d-f. The presence of thermal mass-induced error is highlighted by the 30 m low-passed filtered curves (green lines) in Figures

1d-f. Strong anomalies exist for both the temperature and conductivity, with a low frequency error O(10^{-1}) °C and (10^{-2}) ms.cm^{-1} for temperature (Figure 1d) and conductivity (Figure 1e) respectively. These errors reflect on the salinity estimation, yielding a maximum error O(10^{-1}) psu (green line in Figure 1f). While the scale of the temperature error will be shown to be exceptional due to the extreme magnitude of the temperature gradient, the order of magnitude for the conductivity error is usual for temperature gradients greater than 0.1°C m^{-1} (section 3). Also, the rather extreme temperature gradients observed in this experiment are not unusual in some of the regions sampled by the marine mammals carrying the tags, such as the Okhotsk Sea (Nakanowatari et al., 2017).

Besides the typically large scaled and long-term thermal mass error, discrepancies of smaller scale and shorter-term are evidenced from the profiles of conductivity difference (Figure 1e) and temperature difference (Figure 1d). These errors do not show clearly on the profiles of temperature and conductivity, but manifest on the salinity profile (Figure 1c), as spikes of O(10^{-2}) psu. Such high frequency error may be caused by the irregular flow within the tag sensors, as contrary to the SBE4 cell, the tag is not fitted with a pump stabilizing the inflow. Contrary to the terminology used in the rest of this paper, salinity results in Figure 1 are expressed in practical salinity unit (PSS-78) to illustrate the direct link between conductivity measurement and salinity estimate. However in the following chapters, all salinity results in the tables, text, and figures will be expressed as absolute salinity in g.kg^{-1} in order to follow the new standard recommendations (McDougall et al., 2012). While the values in an absolute salinity profile are generally shifted by ~0.16 compared to those of a practical salinity profile, our correction scheme yields nearly identical results whether conducted on practical or absolute salinity profiles.

2.3. An independent correction scheme for salinity

As a preliminary test, both the conductivity and temperature profiles of each of the 4 tags were corrected using (1) and (2) respectively, with the arbitrary values $\alpha_C = 0.05$, $\alpha_T = 0.037$ and $\beta = 1/30$ s^{-1}. This test produced a significant reduction of the error (not shown) for the temperature, conductivity and salinity data of profiles such as the one displayed in Figure 1. However, correcting the temperature and conductivity separately may lead to an ambiguity in the correction of the salinity estimate. Residual discrepancies may remain due to various causes, e.g. misestimate of the coefficient values for the thermal mass correction or slight misalignment of the CTD and tag pressures, making it possible for the temperature and conductivity residual errors to compensate each other, and to yield a correct salinity estimate. Thus, the search for optimal correction coefficients for temperature and conductivity would be hampered by such considerations. Also, the error in salinity of O(10^{-2}) to O(10^{-1}) g.kg^{-1} is generally between one order below and the same order of magnitude as the salinity variations within any given cast. In contrast, the temperature error is most often of O(10^{-2}) °C, which is two to three orders of magnitude below the typical variations observed within one profile, making the error signal less evident to detect and to correct following the methods described in the next section.

For the sake of practicality, finding a way to correct the salinity estimate directly becomes necessary, and a correction scheme based on (1) could be implemented following the small-amplitude assumption that the salinity correction is a linear combination of the effect of conductivity and temperature corrections:

$$S_T = \frac{\partial S}{\partial C}_{T,p} C_T + \frac{\partial S}{\partial T}_{C,p} T_T \qquad (3)$$

As the causes of the temperature and conductivity thermal mass are similar, we may assume that the time constant β^{-1} which are included in the correction schemes (1) and (2) are identical and we can establish the following salinity correction:

$$S_T(n) = \Gamma_S \alpha (1 - 0.5\beta\Delta_t)^{-1} T_{HP}(n) \quad (4),$$

where $\Gamma_S = \frac{\partial S}{\partial T}_{C,p}$ is the coefficient of sensitivity of salinity to temperature, at fixed conductivity and pressure. The validity of (4) is ensured if within the range of salinity measured, the deviation of Γ_S is small. This is demonstrated in Figure 2a and 2b, which display the values of Γ_C (coefficient of sensitivity of conductivity to temperature) and Γ_S at various values of temperature and conductivity (salinity), respectively. Applying temperature and conductivity corrections following Eq. (1) and Eq. (2) is equivalent to directly correcting salinity using Eq. (4) with an error magnitude $\alpha = \alpha_T - \alpha_C$. One major drawback of correcting directly salinity instead of temperature and conductivity separately, however, is that it might lead to uncorrected biases in both the temperature and density. The magnitude of residual density errors will be discussed later in the study.

3. Results

3.1. Optimized correction coefficients

a. Determination of coefficients

We collected data from 6 different calibration cruises, thereafter called "experiments" during which a set of tags is attached to a CTD frame and conduct profiles simultaneously with a SBE9 CTD system, used as a reference. During each of the experiments, the tags were positioned upward (i.e. the temperature and conductivity sensors facing up) about 50-100 cm above the

CTD, which was installed horizontally at the bottom of the CTD rosette. The profiles are compared during the upcast only, in order to match the in-situ profiling conditions during which the tags are deployed over the head of marine mammals. One drawback in using upcast data however, is that the CTD frame, being a source of turbulence, may generate minor discrepancies when comparing data acquired by tags and CTD. Both CTD and tags data are processed following their respective standard post-processing procedure, the tags temperature and conductivity sensors pressure-dependent drift being previously corrected via the method of Roquet et al. (2011). We call "error" the root mean square (RMS) difference between the salinity obtained from the CTD and that obtained from the tags, and this is calculated before and after implementation of the correction scheme. The salinity correction delineated by Eq. (4) is tested through a least square regression scheme, in which we look for the pair $\alpha_{opt}, \beta_{opt}$ which minimizes the RMS error in salinity $F(\alpha, \beta)$, where,

$$F(\alpha,\beta) = \sqrt{\frac{1}{N \times nc} \sum_{i=1}^{i=nc} \sum_{z=1}^{z=N} \left(S_{ref}(z,i) - S_{tag}^{\alpha,\beta}(z,i) \right)^2} \quad (5).$$

The test was carried out separately for each of the *n* tags in order to obtain a set of optimum correction coefficient α and β; $z=1,2 \ldots N$ is the maximum depth of the measurement (in dbar) and $i=1, 2, \ldots nc$ is the number of casts tested on a given tag. Prior to carrying out the least square regression, all temperature and salinity profiles went through a low-pass filter with a cut-off value set at 10 m, thus avoiding the RMS difference to include high-frequency errors unrelated to thermal mass. During these 6 different experiments, a total of 113 profiles belonging to 42 tags were tested. Experiments *Boussole08* and *Boussole09* were conducted in the western Mediterranean Sea at the BOUSSOLE mooring location in June 2008 and November 2009, respectively. Both of these experiments present strong thermoclines where the time temperature

gradient largely exceeds 0.1 °C.s^{-1}, and where tags data are expected to exhibit strong signs of thermal mass errors. Experiment *Carols08* was conducted in the Bay of Biscay in November 2008 and presents only a moderate thermocline due to the strong winds occurring in the eastern Atlantic in the late autumn. Experiments *Albion08* and *Albion09* were conducted during the Austral summer in the Dumont d'Urville Sea, off the coast of Terre Adelie, Antarctica, and experiment *iStar14* occurred in the Amundsen sea, Antarctica in February 2014. The environment for the latter three experiments is characterized by water temperature between -1.8 °C and +2 °C and generally weaker temperature gradients than those encountered during the Mediterranean Sea or the Bay of Biscay experiments. Of these three experiments, *iStar14* present the largest gradients, with maximum values around 0.1 °C.s^{-1}. The values of the maximum temperature gradients (smoothed over a 10 m window) encountered during each of these experiments are indicated in Table I. We also introduce in this table the value of the maximum high-passed temperature, T_{HP} (Eq. 1, Eq. 4), which can be interpreted as the cumulated effect of the thermal mass on the conductivity sensor. In fact, the thermal mass effect may be more important for a profile where a weak temperature gradient is met by the sensors for a long time/distance, than during a cast where a greater gradient occurs over a shorter time or distance. T_{HP} therefore enables the combined effect of the temperature gradient and its duration to be appropriately expressed. The variable T_{HP} depends on the value of β (section 2.1 and Eq. A4) and throughout this paper we calculate T_{HP} with $\beta = 0.060$ s^{-1}, this being the generic value found for coefficient β (section 3.2).

b. Effects of the correction on salinity data

The value of optimum correction for each of the different experiments are indicated in Table I, where the correction D is defined as $D = F(0,0)_{\mathrm{MaxT_{HP}}} - F(\alpha,\beta)_{\mathrm{MaxT_{HP}}}$, $F(0,0)$ being the

RMS difference between the CTD salinity and the uncorrected tag salinity, and the suffix $MaxT_{HP}$ indicates that F was calculated within ±50 m of the maximum T_{HP}. Thus the effect of the correction is evaluated where the maximum thermal mass error is expected to be. A positive (negative) value of D indicates an improvement (degradation) of the data quality. Figure 3 presents typical CTD, uncorrected and corrected tag profiles for each of the six experiments. The range of salinity error $F(0,0)$ is large, varying between $O(10^{-3})$ g.kg^{-1} and $O(10^{-2})$ g.kg^{-1} depending on the experiment. In particular for the *Boussole08* experiment -where the highest T_{HP} were encountered- the RMS error reaches values as high as 0.053 g.kg^{-1} and the maximum error within a profile exceeds 0.1 g.kg^{-1} (Figure 3f). Conversely, the two *Albion* experiments, with their weaker temperature gradients and T_{HP}, exhibit the smallest RMS error (0.009 g.kg^{-1} and 0.012 g.kg^{-1} respectively). Our results suggest that large discrepancies between tag and CTD can be expected for T_{HP} values exceeding ~1 °C (Table I). These discrepancies are largely reduced for the three experiments presenting the highest T_{HP} values by the correction scheme of (Eq. 4) used with optimally tuned coefficients, with a correction amounting for at least 25% and up to 62% of the original error. This implies that a large part of the error for high T_{HP} experiments is due to thermal mass and that it is effectively removed by the correction scheme adopted here. Conversely, the other three experiments see only a small error decrease, suggesting that most of their RMS difference is due to issues unrelated to thermal mass. In particular for the *Albion08* and *Albion09* experiments, the very low RMS difference and optimal correction value of $O(10^{-3})$ g.kg^{-1} indicate that a RMS difference of ~0.01 g.kg^{-1} represents a nearly irreducible error, considering the accuracy of the tag and CTD sensors. Note that following this optimal coefficient test, 9 out of the 113 profiles tested are found to show insignificant correction in spite of a large

initial error. These large error profiles are assumed to be affected by non-thermal mass related error and are excluded of the analysis in subsequent sections.

c. Optimum coefficient values

The optimum coefficient values vary depending on the experiment, with experiment averaged initial error α ranging between 0.9% and 8.4% and the relaxation time ($1/\beta$) ranging between 11 s and 170 s. The reason for the particularly large range of values for the coefficients is unclear although all but one (*Boussole09*) experiment suggests that α and $1/\beta$ compensate each other, i.e. when the initial error is high (low), the relaxation time is short (long). This compensation between the two coefficients is confirmed later (section 3.2.c and Figure 6) and likely causes a large range of coefficients to yield nearly equal corrections, hence the various values found in Table I. In addition, the properties of the environment in which profiles are conducted could also be partly responsible for the coefficient values. To explore this possibility, we test the ability to predict the values of α and β from environmental predictors. First, coefficients optimized for each individual profiles following (Eq. 5) are estimated, yielding 104 pairs of α_{ind} and β_{ind}. Then predicted values of α are fitted linearly with 10 environmental predictors obtained from each profile according to:

$$\alpha_{\mathrm{pred}}(n) = b_0 + b_1 \mathrm{X}_1(i) + b_2 \mathrm{X}_2(i) + \cdots + b_{10} \mathrm{X}_{10}(i) + \varepsilon(i) \qquad (7)$$

Here, the coefficients b_0 to b_{10} are solved by minimizing the sum of residuals squared $\varepsilon(i)^2$. X_1 to X_{10} correspond to the 10 following environmental predictors: maximum T_{HP}, depth and temperature of the maximum T_{HP}; maximum, mean, and standard deviation of the temperature gradient, minimum, maximum and mean temperature, and mixed layer thickness. A similar operation is conducted for β using the same environmental predictors. Results show that the

297 predicted values α_{pred} and β_{pred} are linearly fitted with α_{ind} and β_{ind} with a coefficient of
298 determination R^2=0.57 and R^2=0.53 respectively. However, if $\alpha_{ind}$is added as X_{11} to determine
299 β_{pred}, the coefficient of determination becomes 0.91. Similarly, if β_{ind} becomes X_{11} in the
300 determination of α_{pred}, the coefficient of determination for the latter becomes 0.92. This
301 highlights the relative importance of the α - β compensation with regards to environmental
302 properties in the profile. To summarize, while α and β compensate each other and an effective
303 correction can be obtained from a large range of coefficient values (section 3.2.c), environmental
304 properties may ultimately decide the best coefficient values within this large range of effective
305 correction coefficients. Following these assumptions on the variability of the coefficients, it
306 seems reasonable that a set of generic coefficients could yield sufficient correction for any kind
307 of profiling environment.

308 3.2. Generic correction coefficients

309 a. Determination of coefficients

310 In order to determine a set of generic coefficients, we adapted the method delineated by
311 (Eq. 5), setting *nc*=60. The *nc* includes 10 randomly chosen profiles from each of the six cruises,
312 in order to avoid a bias generated by the different number of profiles tested during each
313 experiment. This test is repeated 200 times and we average these 200 pairs of α and β
314 coefficients to obtain our generic coefficients. The coefficients obtained via this method are
315 $\alpha_{gen} = 0.041$, and $\beta_{gen} = 0.060$ s^{-1}, or an initial error of 4.1 % and a relaxation time of ~ 17 s, and
316 yield an average correction of 0.011 $g.kg^{-1}$ out of an original averaged error of 0.035 $g.kg^{-1}$.

317 b. Effects of the generic correction on salinity data

The set of generic coefficients performs particularly well for the *Boussole08* dataset which exhibit the strongest temperature gradient. In this case, around 50% of the error is resorbed through the use of generic coefficients, figure which compares well with the ~60% error decrease obtained with the optimum coefficients. Aside from this experiment, the improvement brought by the generic coefficients is more modest but still significant when the initial discrepancy is high. The salinity data from *Boussole09* is corrected by about 20% (Table I) and while the average value of correction for the profiles of the *Carols08* experiment is null, a large number of these profiles are well corrected by the generic coefficients (Figure 3e). The high standard deviation for the correction of the *Carols08* experiment demonstrates however that the changes brought to the profiles are unequal in quality depending on the tag it applies for. On the lower end of the salinity error range, the generic set of coefficient yields either insignificant improvement or, in the case of *Albion08,* a moderate degradation of the data. In this case, illustrated in Figure 3a, the maximum discrepancy of ~0.03 $g.kg^{-1}$ is reached around the halocline at 45 m depth and indicates an overshoot of the correction. This overshoot is resorbed following the halocline as the tag and CTD profiles converge from ~40 m depth to the surface. Some profiles of the *Carols08* experiment follow a similar pattern of degradation.

To further asses the performance of the generic coefficients on this dataset, the values of uncorrected and corrected salinity error - as defined in Table 1 - for each individual profile, are sorted according to their maximum T_{HP}, and averaged per T_{HP} bins of 0.5 °C. The results of this experiment, displayed in Figure 4, demonstrate that the correction performance for T_{HP} values lesser than 2.0 °C is null on average, and with a particularly low standard error. The RMS error increases sharply for the uncorrected data beyond this T_{HP} value, and systematically exceeds 0.05 $g.kg^{-1}$. The RMS error for the salinity corrected with the generic coefficient is strongly reduced

however, and for each T_{HP} bin, generally becomes half the value of the original error. The results in Figure 4 demonstrate that the correction applied with generic coefficient does not degrade the data when a correction may not be needed (very low T_{HP}) and significantly improves the data quality otherwise. Besides slightly degraded profiles such as in Figure 1a, phenomenon independent of the correction performance may lead to an apparent degradation of the data in statistics of the two *Albion* experiments. Since high-frequency errors have been eliminated by the use of a 10 m low-pass filter prior to all our statistical tests, a likely cause could be a slight misalignment of the CTD and tag pressure sensors, or slight changes of positioning of the tags in between some of the casts. Such misalignment may lead to the temperature and salinity profiles being slightly offset, which could artificially cancel the effect of a small thermal mass error, or conversely artificially inflate the error of properly corrected profiles. The case study in section 4 will enable the performance of the generic coefficients in situation of low T_{HP} values to be more accurately evaluated.

c. Impact of generic correction on density error

In order to assess the potential contribution of uncorrected thermal lag errors of the temperature sensor on the density results, we estimate the values of RMS error for the raw and corrected density profiles (Table I). For all but one experiment the density error in $kg.m^{-3}$ is close to the salinity discrepancy in $g.kg^{-1}$, therefore it seems reasonable to assume that the salinity contribution to the density error largely dominates that of temperature. To confirm this assumption, the density error for each individual profile is converted to an equivalent salinity error after calculation of the coefficient of sensitivity of density to salinity, at fixed temperature and for a change of salinity of ±0.5 $g.kg^{-1}$, $\Gamma_\rho = \frac{\partial \rho}{\partial S_T}$. This coefficient value is close to 0.77 for all

the tags, which means that if salinity varies by 1 g.kg^{-1}, density will see a change of ~0.77 kg.m^{-3}. The equivalent salinity error S_{Eq} is then obtained by dividing each profile density error by its Γ_ρ coefficient, and is subsequently plotted against the actual salinity error RMS_S (which equals $F(0,0)_{\mathrm{MaxT_{HP}}}$) on Figure 5a. On this figure is also plotted a line of equation $y = \frac{1}{0.77}x$ which represents the value that should take S_{Eq} if it is entirely caused by RMS_S. Points located above (below) that line present a negative (positive) temperature error proportional to the vertical distance between the equivalent salinity error and the line. The Results from this figure show that most of the points with a salinity error lesser than 0.03 g.kg^{-1} fall very close to the *y* line, thus confirming that the temperature error has little significance in those cases. For errors larger than 0.03 g.kg^{-1}, those profiles with T_{HP} values greater than ~2 °C (largest dots in Figure 5a) present a significant temperature error, as shown by the large vertical distance between the line and the dots on Figure 5a. For each profile, the percentage of density error due to temperature ε_T can be calculated from this vertical distance via

$$\varepsilon_T = \left(S_{Eq} - \frac{RMS_S}{\Gamma_\rho}\right)/S_{Eq} \qquad (6)$$

For each profile, the RMS density error and ε_T are used to obtain a value in kg.m^{-3} of density error due to temperature, E_T . Both E_T and ε_T are plotted against T_{HP} in Figure 5c and these results demonstrate that significant density error (due to temperature) can be found only for profiles whose maximum T_{HP} values exceed 2 °C, which corresponds to temperature gradients around 0.20 – 0.28 °C s^{-1}. In these cases E_T values greater than 0.01 kg.m^{-3} and amounting for ~20-30% of the total density error are expected.

Results for the data corrected with the generic coefficients show a general decrease of the salinity and equivalent salinity errors, demonstrating that the correction scheme adopted here with a generic set of coefficient improves both salinity and density estimations. In those cases where E_T is large on the uncorrected profiles, the equivalent salinity error also decrease after correction due to the role of the salinity correction scheme, but the temperature-related errors remain essentially unchanged as can be seen from the large vertical distance between each dot and the *y* line (Figure 5b).

d. Generic correction coefficient values

Figure 6 displays the amount of correction for any pair of coefficients located within a large interval of α and β. The values of the generic set of coefficients ($\alpha_{gen} = 0.041$, $\beta_{gen} = 0.060$ s^{-1}) and each optimum coefficients for individual profiles are also displayed on the figure. This graphic allows to see a large beam - whose limits are defined by the 0.010 $g.kg^{-1}$ isoline- within which pairs of coefficients yield a correction close to α_{gen}, β_{gen}. We can therefore assume that the generic coefficients will provide a correction close to the optimum correction for those profiles whose α_{ind}, β_{ind} are within the high-correction beam. This is the case for nearly half the profiles of Boussole08 and a third of *Carols09* profiles. This should also be the case for the Nakanowatari et al. (2017) experiment, where the pair of optimum coefficient ($\alpha_{Okh} = 0.05$, $\beta_{Okh} = 0.06s^{-1}$) was determined via a comparison of tag data and historical data from the WOA13 in the Okhotsk Sea, and yield a decrease of salinity error of 0.07 psu over the uppermost 20 m of the water column. In contrast, those profiles whose α_{ind}, β_{ind} are located far from this beam will see the generic coefficients perform notably less well compared to the optimum correction. Note that contrary to the per-experiment statistics, the individual profiles statistics show a trend where profiles with $T_{HP} < 2.0$ °C (empty symbols on Figure 6) are generally

corrected by small values of α and β while profiles with large T_{HP} values and error tend to be corrected by large values of α and proportionally large values of β. Also, 26 profiles are located out of the figure limits, with nearly two dozen coefficient pairs of low T_{HP} profiles having a slightly negative value of α or β. This fact illustrates the difficulty to determine correction coefficients for very low T_{HP} conditions where little or no thermal mass error exists and where other errors might hamper the determination of coefficients. This issue is essentially solved when optimum coefficients are calculated per tag instead of individual profiles. While the variety of optimum coefficients should encourage users to determine their own optimum coefficients in the areas of deployment whenever possible, this is often not possible or ideal as the seals may travel long distances throughout the deployment period and seasonal changes of water properties will also change the profiling environment. Our results have shown that the use of a set of generic coefficient provides satisfactory results for the conditions of the 6 aforementioned experiments, and the case study in the next section will further demonstrate the ability of this set of coefficients to provide an effective correction in operational conditions even when the T_{HP} is low.

4. Application of the generic correction to CTD-SRDL bio-logged data

4.1 Dataset

The thermal lag correction scheme described in (Eq. 4) and with the generic coefficients ($\alpha_{gen} = 0.041$, $\beta_{gen} = 0.060$ s^{-1}) is applied to 5 full-resolution CTD-SRDL tags deployed on Southern Elephant Seal (SES) around the Kerguelen Islands in the Indian sector of the Southern Ocean during the austral summer. A unique dataset made of full-resolution CTD-SDRL hydrographic profiles acquired by 5 female SES from October 2014 to January 2015 has been used to test the robustness and efficiency of the thermal lag procedure and generic coefficients.

Full-resolution tags record temperature, salinity and pressure at a frequency of 0.5 Hz for every dive of the seal's journey. Besides the high resolution of this dataset, another advantage resides in the acquisition of both ascending and descending phases for every dive, which allows comparison of the data and evaluation of the correction to be done. The environment in which the SES conducted profiles is marked by low temperatures and mild temperature gradients, successively negative between 0 and 150 m, then positive between 150 m and 350 m (Figure 7a). Accordingly, these weak temperature gradients are associated with weak T_{HP} values with the 20th -80th percentile envelope ranging between -0.17° C and 0.22° C (Figure 7c). This place this datasets below most of the T_{HP} values tested in the six experiments described earlier. Steady salinity changes occur throughout the water column.

4.2 Implementation of the correction

The thermal lag procedure was applied on the ascending and descending phases of every dive. A total of 22308 dives ranging from depths of minimum 150 up to 1000 m have been used. The ascending phase of any *n* dive is then compared to the descending phase of dive *n*+1 for dives occurring within a 5 minutes interval in order to compare similar water masses. For each tag, the RMS error of ascend vs. descend is first calculated at each depth *z* according to:

$$RMS_{ad}(z) = \sqrt{\frac{1}{np}\sum_{n=1}^{n=np}\left(S_a(z,n) - S_d(z,n+1)\right)^2} \qquad (8)$$

with *np* the total number of dives, and S_a and S_d the salinity during the ascent and descent respectively. RMS_{ad} is calculated for both the uncorrected ($RMS_{ad_{raw}}$) and corrected ($RMS_{ad_{cor}}$) versions and show values between ~0.02 and 0.03 g.kg^{-1} for all but one tag (Table II). These relatively large values are in most part not due to the thermal lag and are likely related to slight

changes in the geographic location of the ascent compared to the descent. The occurrence of a relatively large temperature RMS for all tags (Table II) in spite of the weak temperature gradients confirms that environmental changes account for a large part of the RMS error. Therefore, the performance of the correction is evaluated through the difference of $RMS_{ad_{raw}}$ and $RMS_{ad_{cor}}$, positive values indicating a decrease of the RMS error. All 5 tags see a significant improvement after the application of the thermal lag correction, where the difference between the ascending and descending phases for both the salinity and density field is minimized, as can be seen from the $RMS_{ad_{raw}} - RMS_{ad_{cor}}$ profile averaged for all tags (Figure 7d). The thermal lag correction impact is more pronounced in the areas where stronger gradients of temperature are located, i.e. between the surface and 300 m depth. The results obtained for this depth range are presented in Table II. RMSs of salinity and potential density are the greatest for tag 35 due to some technical issues flagged with the salinity sensor of this particular tag and independent of the thermal lag procedure. This issue does not affect the values and profile of $RMS_{ad_{raw}} - RMS_{ad_{cor}}$. Besides the averaged effect of the correction procedure over the water column presented in Figure 7d, a typical pre and post-correction profile is shown in Figure 8. The profile which occurs in a region presenting sharper temperature variations sees its salinity difference between ascent and descent reduce by nearly 0.04 $g.kg^{-1}$, a rather considerable improvement which is also reflected on the density profile (Figure 8c) and on the TS plan (Figure 8d).

5. Summary and conclusion

The SRDL-CTD tag sensors are subject to the thermal mass phenomenon which affects other conductivity cells such as the Seabird Scientific © SBE4. This paper has documented the

effect of thermal inertia on the tags conductivity cell and provided evidence of thermal mass induced errors increasing with the magnitude of the temperature gradient, and more specifically with the magnitude of the cumulated effect (T_{HP}) of temperature gradient within a profile. The thermal mass applying on the conductivity cell reflects as a significant error in salinity estimates. Salinity error -defined here as the root mean square difference between a standard CTD upcast and a concurrent tag profile- amounting for ~0.02 $g.kg^{-1}$ for $T_{HP} < 2$ °C and >0.05 $g.kg^{-1}$ for larger T_{HP}, occurs. A correction scheme was therefore developed to improve the salinity estimates. The main part of the correction methodology is a further development of the conductivity correction scheme of Lueck (1990), where correction coefficients represent the initial measurement error α and the inverse relaxation time β. However, the tag's temperature sensor is also affected by thermal mass, which implies that to obtain an accurate estimate of salinity, both the conductivity and temperature data are to be perfectly corrected simultaneously. For practical reasons described further in this section, this is difficult to achieve and thus we developed a correction algorithm to be applied directly on salinity. The correction algorithm is successfully implemented and tested on 42 different tags profiling in various hydrographic conditions and experiencing different ranges of temperature gradients, T_{HP} and error. Comparison between tag and CTD profiles conducted simultaneously allowed to calibrate the coefficients α and β for each of the tags. These optimum coefficients systematically lead to a significant improvement for all tags whose T_{HP} is 2 °C or above, with an error decrease of up to 60%. However, the range among which these optimal coefficients varies is large, suggesting a compensation effect between the magnitude of the initial error α and the relaxation time $1/\beta$, with possible further influence from the environment in which a given profile is conducted. A generic set of correction coefficients was therefore determined to account for the coefficients

variability. This set of coefficients ($\alpha_{gen} = 0.041$, $\beta_{gen} = 0.060$ s^{-1}) yields an error decrease of nearly 50% for those profiles with a T_{HP} greater than 2 °C (the latter which on average corresponds to temperature gradients of 0.20 – 0.28 °C.s^{-1}). Results for lower T_{HP} or gradients were less clear due to intrinsic difficulties in evaluating small errors in CTD vs. tag experiments, and to further assess the performance of α_{gen} and β_{gen}, more than 22000 profiles acquired from 5 different tags deployed in the Southern Ocean were evaluated. The difference in salinity between each downcast and upcast was used to assess the effectiveness of the generic coefficients, and was found to reduce on average by 0.006 g.kg^{-1} for profiles whose maximum T_{HP} was extremely low with averaged values of ~0.1 °C. Those profiles presenting larger T_{HP} or temperature gradients saw very significant improvements with examples of upcast-downcast salinity difference reducing from 0.06 g.kg^{-1} to 0.02 g.kg^{-1}. Both this test and the CTD vs. tags experiments demonstrate that the salinity correction leads to a substantial decrease of the density error.

Besides the effects of thermal mass on conductivity measurements/salinity estimates, temperature measurements also appear to be affected by thermal mass induced errors. Temperature discrepancies are insignificant for $T_{HP} < 2$ °C but become large for $T_{HP} > 2$ °C, amounting for about ~25% of the error in density. While temperature gradients in excess of 0.20 – 0.28 °C.s^{-1} (which is roughly equivalent of a T_{HP} of 2 °C) are less frequently met in the ocean, they do still occur in some of the areas typically sampled by tag-equipped mammals (Nakanowatari et al., 2017), and call for an appropriate correction. However, the rather high limit above which the temperature error becomes significant (limit met by only 24 profiles), combined with a larger sensitivity of the least square regression scheme used to determined correction coefficients make our dataset inadequate to define correction coefficients for temperature. Future

development for the improvement of the temperature data requires a larger number of profiles acquired in high T_{HP} conditions as well as perfectly aligned pressure measurements for the tag and CTD used in the experiments.

Another possible improvement of the correction scheme could consist in adapting the correction coefficients according to the ascent velocity of the tag, as was done in Liu et al. (2015) for glider data. Different profiling speeds are expected to be met depending on the species or body condition of the mammals on which the tags are deployed, and these are likely to affect the value of the coefficients. However, as the results of Figure 6 suggest, the range within which the correction yield similar results is large, allowing for performances of the generic coefficients to be satisfactory even when the profiling speed differs significantly from ~ 1 $m.s^{-1}$.

It is noteworthy that while the scheme described in this study applies directly on salinity data, the generic coefficients found here can be used to correct the conductivity following (Eq. 1) and using $\alpha_C = -\alpha_{gen}$ and $\beta_c = \beta_{gen}$, following the assumptions developed in section 2.3. A test has been conducted on the data from the 6 above-mentioned experiments and yield insignificant differences between the conductivity and salinity versions of the correction. It was however crucial to use the salinity to determine our coefficients in this study. The nature and relative magnitude of the salinity error indeed made this determination more robust than using conductivity, whose signal and error are correlated with those of temperature. Lastly, while this paper documents the effects of our correction scheme on full-resolution tags data (1 or 0.5 Hz sampling rate), most of CTD-SRDL profiles available to date are heavily compressed due to satellite transmission constraints with a typical number of 20 data points per temperature/salinity profile (Boehme et al. 2009). The slow response nature of the thermal mass effect, and the low-pass filtering conducted on the data for the tags vs. CTD test make it highly likely that the

correction will be useful on low-resolution salinity data. Nakanowatari et al. (2017)'s work is an example of the successful implementation of this thermal mass correction algorithm on post-processed low-resolution data in the Okhotsk Sea. Users are therefore encouraged to apply the thermal mass algorithm on their low-resolution salinity data, which should yield a significant reduction of the thermal mass induced-errors.

Appendix I: Equivalence between the Lueck and Picko (1990) recursive filter and a standard first-order high-pass filter

Here it is shown that the recursive filter scheme devised by Lueck and Picko (1990) to correct the thermal mass effect on a measured variable X (conductivity in their case) is formally equivalent to a standard first-order high-pass filter applied on the temperature discrete signal, once suitably rescaled.

The recursive filter of Lueck and Picko (1990) is given by,

$$X_T(n) = -bX_T(n-1) + \Gamma_X a[T(n) - T(n-1)], \quad \text{(A1)},$$

where X_T is the correction of conductivity added to the conductivity of the nth sample, T is the sample's temperature, n is the sample index, Γ_X is the sensitivity of X to temperature, and a and b are coefficients depending of α and β according to:

$$a = \alpha/\left(1 + 0.25\beta {f_n}^{-1}\right) \quad \text{(A2)}$$

and

$$b = 1 - 2a\alpha^{-1} \quad \text{(A3)}$$

where $f_n = (2\Delta_t)^{-1}$ is the Nyquist frequency function of the sampling interval Δ_t.

Define the high-pass filtered temperature signal T_{HF} as,

$$T_{HP}(n) = \frac{\tau}{\tau+\Delta_t}[T_{HP}(n-1) + T(n) - T(n-1)], \quad \text{(A4)},$$

where τ is the time constant of the filter. Assuming that the correction is proportional to the high-pass filtered temperature signal, $X_T = AT_{HP}$, and neglecting variations of the factor A between two consecutive samples (an excellent assumption in practice, see Figure 2), a relation can be found between equations (A1) and (A4) providing the two identities $b = -\tau/(\tau + \Delta_t)$ and $A = \Gamma_X \alpha(1 + \Delta_t/\tau)$. Using equations (A2) and (A3) and after some rearrangement, it comes that the recursive filter of Lueck and Picko (1990) is strictly equivalent to rescaling the high-pass filtered temperature signal T_{HP}using a time constant $\tau = \beta^{-1} - 0.5\Delta_t$ and a factor $A = \Gamma_X \alpha(1 - 0.5\beta\Delta_t)^{-1}$.

Note that the filter is defined only if $\beta^{-1} > 0.5\Delta_t$, and that in the limit case $\beta\Delta_t \ll 1$, the time constant of the filter tends toward $\tau = \beta^{-1}$ and the correction simply tends toward $X_T = \Gamma_X \alpha T_{HP}$.

Acknowledgments

The present study is a contribution to the SO-MEMO (Observing System – Mammals as samplers of the Ocean Environment) with funding and logistic support from CNES-TOSCA, IPEV and CORIOLIS in-situ ocean observation program. We are very grateful to D. Antoine for giving us access to the R/V Tethys II, G. Reverdin for access to the R/V Cotes de la Manche and M.-N. Houssais for access to the R/V L'astrolabe data. The iStar14 data, obtained on the R/V RSS James Clark Ross during the iSTAR JR294/295 cruise, were kindly made available to us by Karen Heywood and Helen Mallett. We also thank two anonymous reviewers for their constructive criticism. We extend our warm thanks to the crews and captains of the different research vessels.

REFERENCES

585 Antoine, D., and Coauthors, 2006: BOUSSOLE: A joint CNRS- INSU, ESA, CNES, and NASA ocean color
586 calibration and validation activity. GSFC Tech. Rep. NASA/TM–2006–214147, 68 pp. [Available online at
587 http://www.obs-vlfr.fr/LOV/OMT/ fichiers_PDF/Antoine_et_al._NASA_TM_boussole.pdf.] Antoine, D.,
588 Guevel, P., Desté, J.F., Bécu, G., Louis, F., Scott, A.J., Bardey, P., 2008. The "BOUSSOLE"buoy—A
589 new transparent-to-swell taut mooring dedicated to marine optics: Design, tests, and performance at sea.
590 Journal of Atmospheric and Oceanic Technology, volume 25(6):pp. 968–989.
591 Boehme, L., Lovell, P., Biuw, M., Roquet, F., Nicholson, J., Thorpe, S. E., Meredith, M. P., and Fedak,
592 M., 2009. Technical Note: Animal-borne CTD-Satellite Relay Data Loggers for real-time oceanographic
593 data collection. Ocean Science, 5:685-695.
594 Garau, B., Ruiz, S., Zhang, W. G., Pascual, A., Heslop, E., Kerfoot, J., and Tintoré, J., 2011. Thermal Lag
595 Correction on Slocum CTD Glider Data. Journal of Atmospheric and Oceanic Technology, 28:1065-1071.
596 Liu, Y., Weisberg, R.H., Lembke, C., 2015. Glider salinity correction for unpumped CTD sensors across
597 a sharp thermocline, Coastal Ocean Observing Systems, 305-325. https://doi.org/10.1016/B978-0-12-
598 802022-7.00017-1
599 Lueck, R.G., 1990. Thermal inertia of conductivity cells: Theory. Journal of Atmospheric and Oceanic
600 Technology, volume 7(5):pp. 741–755.
601 Lueck, R.G., Picklo, J.J., 1990. Thermal inertia of conductivity cells: Observations with a Sea-Bird cell.
602 Journal of Atmospheric and Oceanic Technology, volume 7(5):pp. 756–768.
603 McDougall, T., Jackett, D., Millero, F., Pawlowicz, R., Barker, P., 2012. A global algorithm for
604 estimating Absolute Salinity. Ocean Science, volume 8(6):pp. 1123–1134.
605 Mensah, V., Le Menn, M., Morel, Y., 2009. Thermal Mass Correction for the Evaluation of Salinity.
606 Journal of Atmospheric and Oceanic Technology, volume 26.
607 Morison, J., Andersen, R., Larson, N., D'Asaro, E., Boyd, T., 1994. The correction for thermal-lag effects
608 in Sea-Bird CTD data. Journal of atmospheric and oceanic technology, volume 11(4):pp. 1151–1164.

609 Nakanowatari, T., K. I. Ohshima, Mensah, V., Mitani, Y., Hattori, Y., Kobayashi, M., Roquet, F., Sakurai,
610 Y., Mitsudera, H., Wakatsuchi, M., 2017. Hydrographic observations by instrumented marine mammals
611 in the Sea of Okhotsk. Polar Science.volume 13 :pp. 56-65.
612 Roquet, F., 2011. Delayed-mode calibration of hydrographic data obtained from animal-borne satellite
613 relay data loggers. J. Atmos. Ocean. Technol., volume 41:pp. 787–801.
614 Roquet, F., Williams, G., Hindell, M. A., Harcourt, R., McMahon, C., Guinet, C., Charrassin, J.-B.,
615 Reverdin, G., Boehme, L., Lovell, P., and Fedak, M., 2014. A Southern Indian Ocean database of
616 hydrographic profiles obtained with instrumented elephant seals. Scientific Data, 1.
617 Treasure, A.M., F. Roquet, I.J. Ansorge, M.N. Bester, L. Boehme, H. Bornemann, J.-B. Charrassin, D.
618 Chevallier, D. Costa, M.A. Fedak, C. Guinet, M.O. Hammill, R.G. Harcourt, M.A. Hindell, K.M. Kovacs,
619 M.-A. Lea, P. Lovell, A.D. Lowther, C. Lydersen, T. McIntyre, C.R. McMahon, M.M.C. Muelbert, K.
620 Nicholls, B. Picard, G. Reverdin, A.W. Trites, G.D. Williams, and P.J.N. de Bruyn. 2017. Marine
621 mammals exploring the oceans pole to pole: A review of the MEOP Consortium. Oceanography
622 30(2):132–138, https://doi.org/10.5670/oceanog.2017.234.

623

Figures captions

Figure 1. CTD-SRDL and reference SBE CTD cast acquired on 11 June 2008 at the BOUSSOLE mooring site. (a) Temperature profiles, (b) conductivity and (c) salinity. Panels, (d), (e) and (f) display the temperature, conductivity and salinity difference (CTD minus tag) between both sensors, respectively. The green line in the right panels represents the 30 m low-passed filter signal. The thermal mass error is characterized by the strong, low frequency anomaly visible above the thermocline within the upper 50 meters.

Figure 2. Values of coefficients (a) Γ_S of sensitivity of salinity to temperature, and (b) Γ_C of sensitivity of conductivity to temperature, for ranges of temperature and salinity (conductivity) typically measured in regions sampled by the tags.

Figure 3. Reference CTD and typical tag profiles for all 6 experiments: a) *Albion08*, b) *Albion09*, c) *iStar14*, d) *Boussole09*, e) *Carols08*, and f) *Boussole08*. The four curves on each panel represent the reference CTD profile (blue), non-corrected tag profile (black), tag profile corrected with a pair of optimum coefficients (red) and tag profile corrected with a pair of generic coefficients (green).

Figure 4: Root mean Square (RMS) difference of reference and tag salinity as a function of the high pass filtered temperature T_{HP}, calculated from all the data points located within ± 50 m of the maximum T_{HP} for the six experiments mentioned in this study. The red and blue curves stand for the uncorrected and corrected data (using the set of generic coefficients), respectively. The error bars represent the standard error of the estimate.

Figure 5. Comparative plot of salinity error vs. equivalent salinity error for each of the 104 profiles tested, (a) errors for uncorrected tags and (b) errors for tags corrected with the set of generic coefficients. The size of the dots represents the magnitude of the maximum T_{HP} observed by each of the tags. The black line with a slope a=0.77 represents the sensitivity of density to salinity, i.e. the change of density caused

by a change of 1 $g.kg^{-1}$ of salinity. The equivalent salinity error is calculated by converting density error into salinity error, with the assumption that the density error is entirely due to a discrepancy in salinity. Data fulfilling this assumption will have their equivalent salinity error located on this line. (c) Density error due to temperature expressed as a percentage of the total density error (blue) and as a value in $kg.m^{-3}$ (black), as a function of the maximum high-passed filter temperature T_{HP}.

Figure 6. Salinity correction for different values of coefficients α and β, with $F(\alpha, \beta)$ calculated within ± 50 m of the maximum T_{HP} of all the casts tested. The limit of null correction is represented with the white isoline and the various symbols represent the values of optimum coefficients for each profiles for all the experiments tested in this study as well as from the experiment conducted by Nakanowatari et al. (2017). Filled symbols represent those profiles whose maximum T_{HP} exceeds 2.0 °C and empty symbols those whose maximum T_{HP} fall below this limit.

Figure 7 (a) Mean Temperature, (b) salinity, (c) T_{HP}, (d) RMS_{ad_raw}-RMS_{ad_cor} profiles averaged for all full-resolution CTD-SRDL tags deployed on SES around the Kerguelen Islands. The shaded area envelopes represent the 20th and 80th percentile in all 4 plots.

Figure 8: A typical ascent (blue) and descent (red) profile comparison closed up view on the upper 300 m: (a) Temperature, (b) salinity, (c) potential density, and (d) TS diagram. On panels (a), (b) and (c), dashed lines represent raw profiles and solid lines represent the corrected profiles. To enhance visibility, a gaussian filter with a 5dbar window was applied on the profiles.

667 Table 1. Salinity correction statistics per experiment: maximum high passed temperature (T_{hp}), error magnitude, values of $\alpha_{opt}, \beta_{opt}$
668 coefficients for each experiment, averaged magnitude for both the optimum and generic correction in terms of salinity and density,
669 with standard deviation indicated between brackets. The error and correction magnitude are calculated within ±50 m of the maximum
670 T_{hp}.

						Salinity (±50 m of maximum T_{HP})			Density (±50 m of maximum T_{HP})		
Experiment	Tags tested (number of profiles)	Ascent speed (m s^{-1})	Maximum temperature gradient (°C s^{-1})	Maximum Thp (°C)	α_{opt} , β_{opt} (averaged)	Error (g.kg^{-1})	Optimum correction (g.kg^{-1})	Generic correction (g.kg^{-1})	Error (g.kg^{-1})	Optimum correction (g.kg^{-1})	Generic correction (g.kg^{-1})
Albion09	7 (21)	1.0	0.06	0.67	0.009, 0.006	0.012	0.000 (0.002)	-0.002 (0.003)	0.010	0.000 (0.002)	-0.002 (0.002)
Albion08	5 (15)	0.75	0.08	0.83	0.009, 0.014	0.009	0.002 (0.002)	-0.003 (0.003)	0.008	0.002 (0.002)	-0.001 (0.003)
iStar14	16 (16)	1.0	0.11	- 0.87	0.046, 0.088	0.023	0.001 (0.006)	0.001 (0.006)	0.019	0.001 (0.005)	0.001 (0.004)
Boussole09	3 (12)	0.35	0.13	1.10	0.062, 0.002	0.022	0.009 (0.011)	0.004 (0.002)	0.022	0.009 (0.006)	0.003 (0.001)
Carols09	7 (21)	1.3	0.18	1.78	0.014, 0.027	0.022	0.005 (0.011)	0.000 (0.021)	0.024	0.005 (0.010)	0.003 (0.017)
Boussole08	4 (28)	0.7	0.47	4.34	0.084, 0.077	0.053	0.033 (0.021)	0.026 (0.012)	0.073	0.036 (0.015)	0.021 (0.004)

671
672
673

Table 2 Statistics for 5 tags deployed on SES in the southern ocean region off Kerguelen islands. Beside RMS_{ad_raw} and RMS_{ad_cor}, other variables include the RMS of temperature, and RMS of potential density. All RMS variables here have been calculated between the surface and 300 m depth.

Tag ID	Number of dives	RMS_T (°C)	RMS_{ad_raw} ($g.kg^{-1}$)	RMS_{ad_cor} ($g.kg^{-1}$)	$RMS_{\_rho\_raw}$ ($kg.m^{-3}$)	$RMS_{\_rho\_cor}$ ($kg.m^{-3}$)	Ascent Velocity ($m.s^{-1}$)	Descent Velocity ($m.s^{-1}$)
33	4689	0.122	0.033	0.028	0.027	0.022	-1.32	1.43
35	1536	0.122	0.086	0.084	0.077	0.075	-1.41	1.52
48	5739	0.103	0.025	0.022	0.020	0.017	-1.37	1.52
49	4950	0.081	0.021	0.018	0.017	0.014	-1.33	1.26
50	5394	0.065	0.020	0.016	0.017	0.013	-1.38	1.29

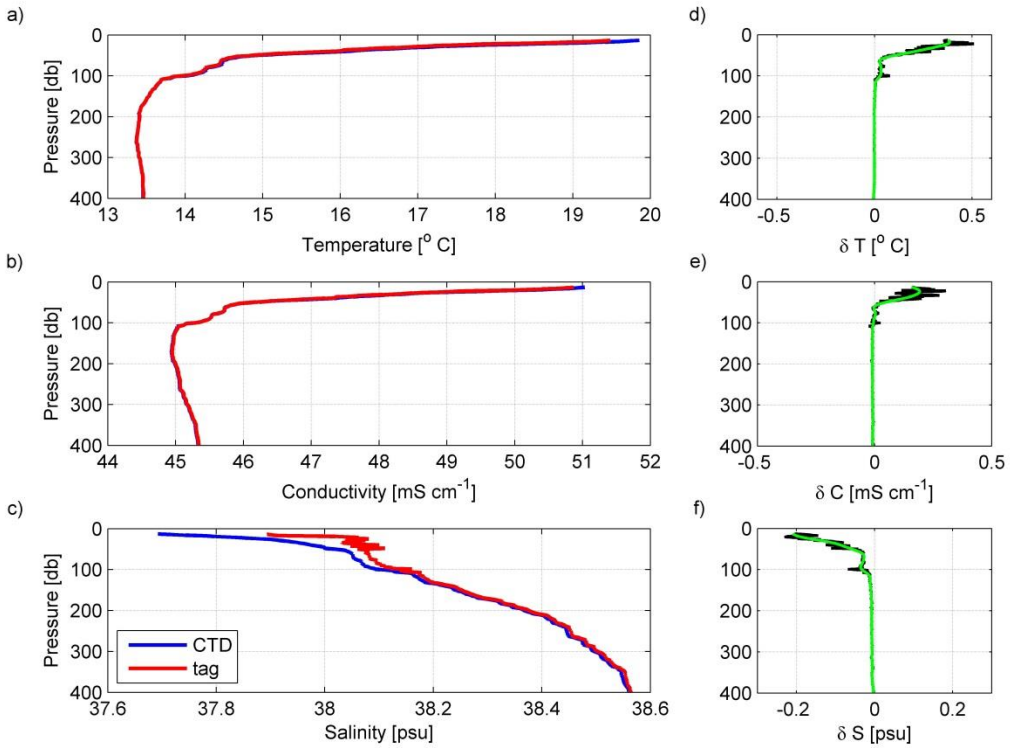

677

678 Figure 1. CTD-SRDL and reference SBE CTD cast acquired on 11 June 2008 at the BOUSSOLE
679 mooring site. (a) Temperature profiles, (b) conductivity and (c) salinity. Panels, (d), (e) and (f) display the
680 temperature, conductivity and salinity difference (CTD minus tag) between both sensors, respectively.
681 The green line in the right panels represents the 30 m low-passed filter signal. The thermal mass error is
682 characterized by the strong, low frequency anomaly visible above the thermocline within the upper 50
683 meters.

684

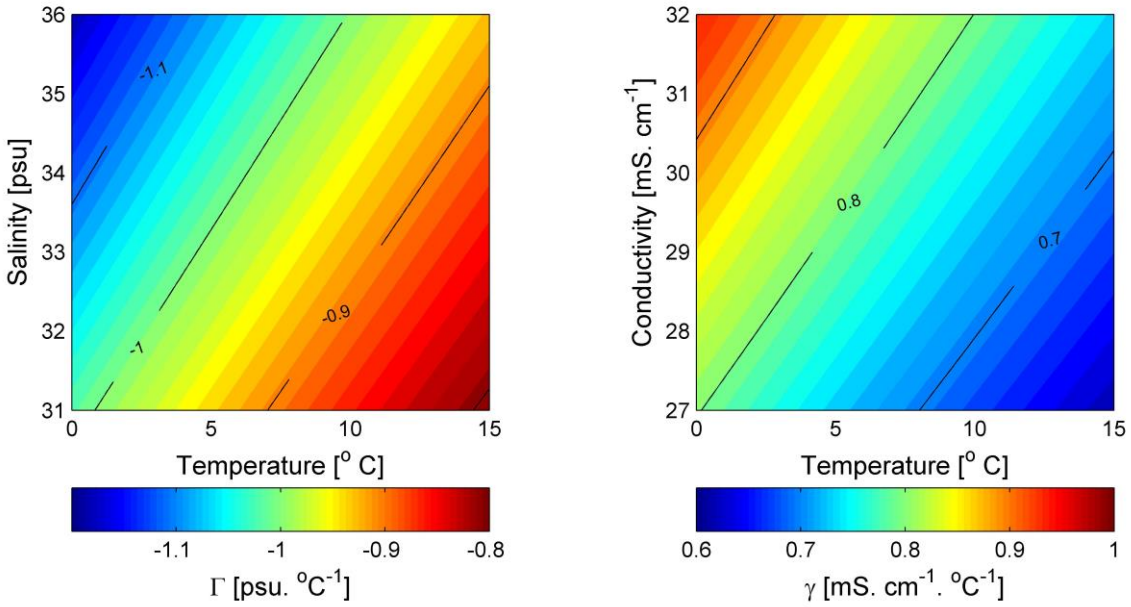

685

686 Figure 2. Values of coefficients (a) Γ_S of sensitivity of salinity to temperature, and (b) Γ_C of sensitivity of
687 conductivity to temperature, for ranges of temperature and salinity (conductivity) typically measured in
688 regions sampled by the tags.

689

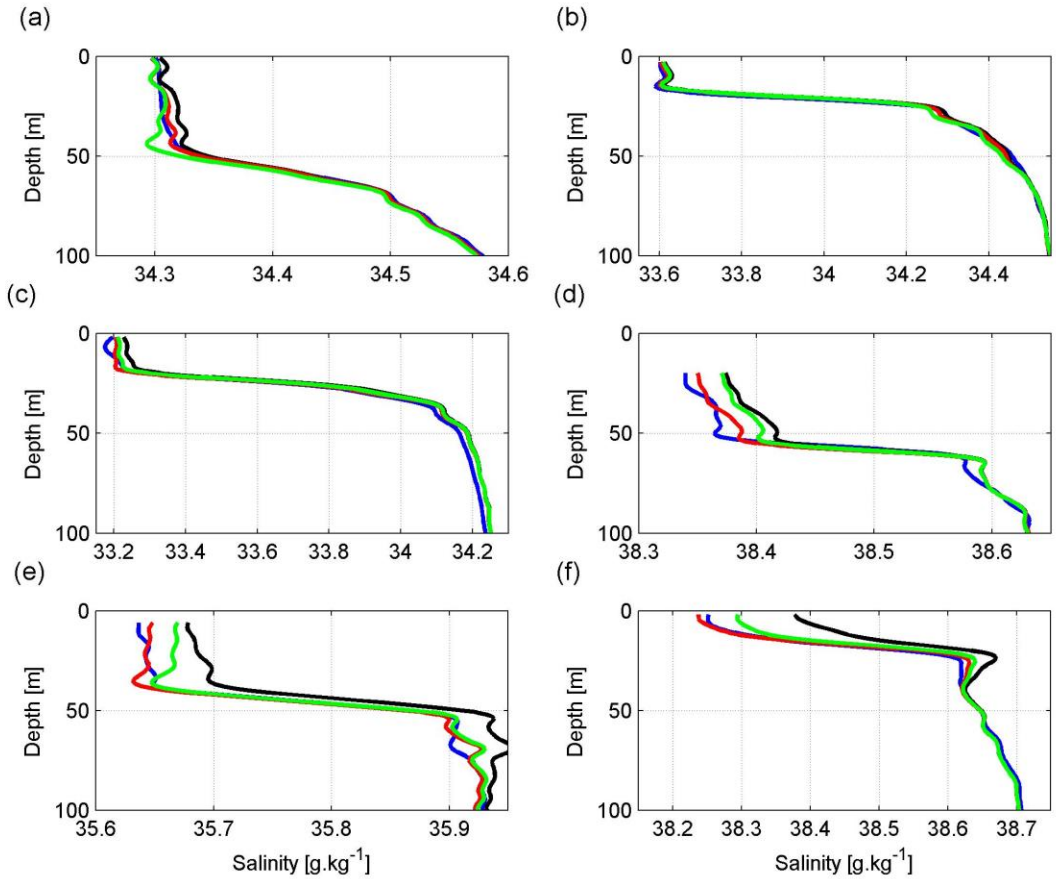

Figure 3. Reference CTD and typical tag profiles for all 6 experiments: a) *Albion08*, b) *Albion09*, c) *iStar14*, d) *Boussole09*, e) *Carols08*, and f) *Boussole08*. The four curves on each panel represent the reference CTD profile (blue), non-corrected tag profile (black), tag profile corrected with a pair of optimum coefficients (red) and tag profile corrected with a pair of generic coefficients (green).

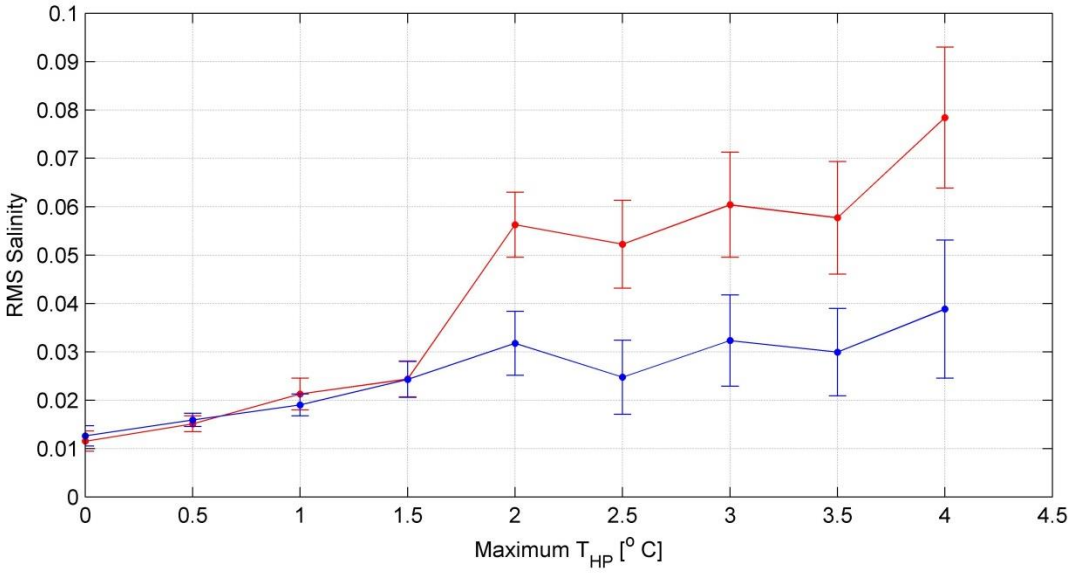

697

698 Figure 4: Root mean Square (RMS) difference of reference and tag salinity as a function of the high pass
699 filtered temperature T_{HP}, calculated from all the data points located within ± 50 m of the maximum T_{HP} for
700 the six experiments mentioned in this study. The red and blue curves stand for the uncorrected and
701 corrected data (using the set of generic coefficients), respectively. The error bars represent the standard
702 error of the estimate.

703

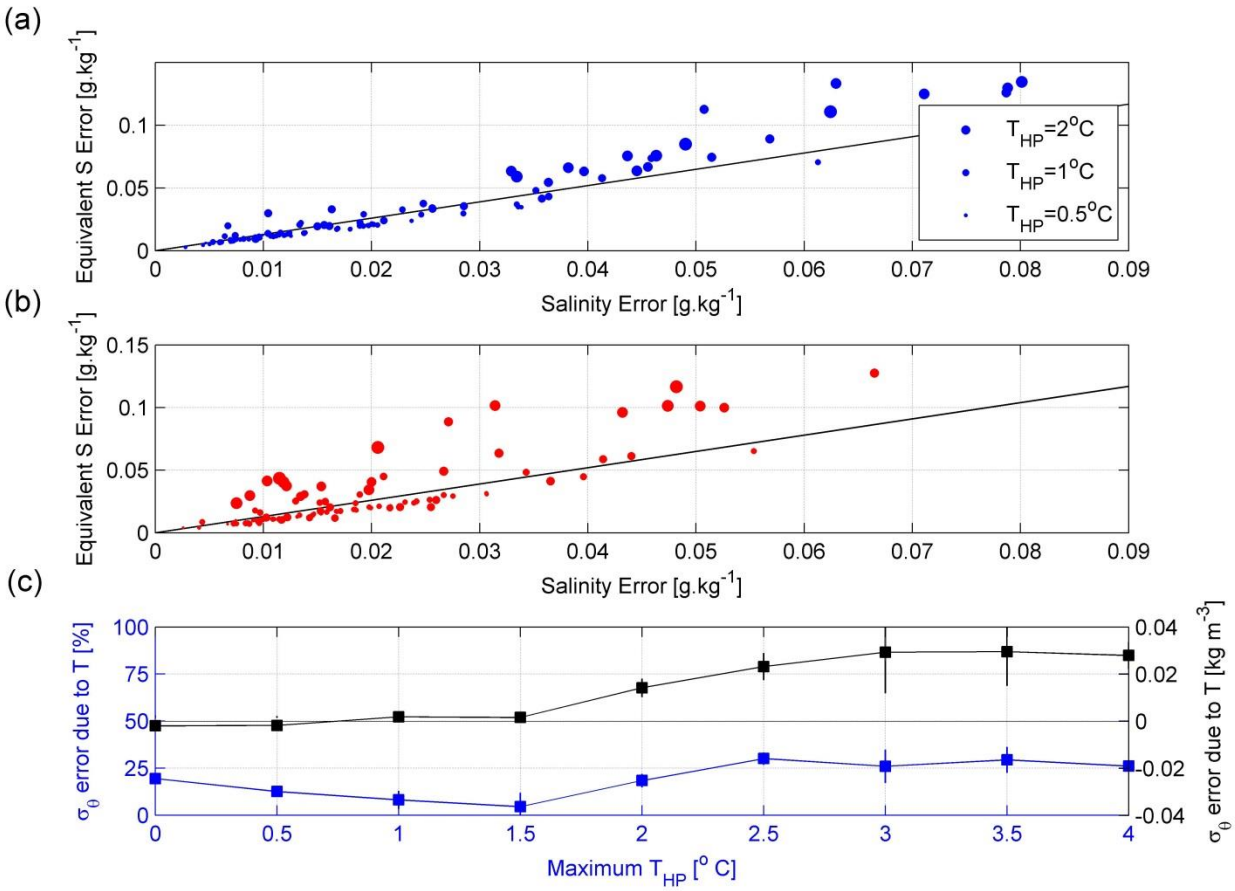

704

705 Figure 5. Comparative plot of salinity error vs. equivalent salinity error for each of the 104 profiles tested,
706 (a) errors for uncorrected tags and (b) errors for tags corrected with the set of generic coefficients. The
707 size of the dots represents the magnitude of the maximum T_{HP} observed by each of the tags. The black
708 line with a slope a=0.77 represents the sensitivity of density to salinity, i.e. the change of density caused
709 by a change of 1 g.kg^{-1} of salinity. The equivalent salinity error is calculated by converting density error
710 into salinity error, with the assumption that the density error is entirely due to a discrepancy in salinity.
711 Data fulfilling this assumption will have their equivalent salinity error located on this line. (c) Density
712 error due to temperature expressed as a percentage of the total density error (blue) and as a value in kg.m^{-3}
713 (black), as a function of the maximum high-passed filter temperature T_{HP}.

714

715

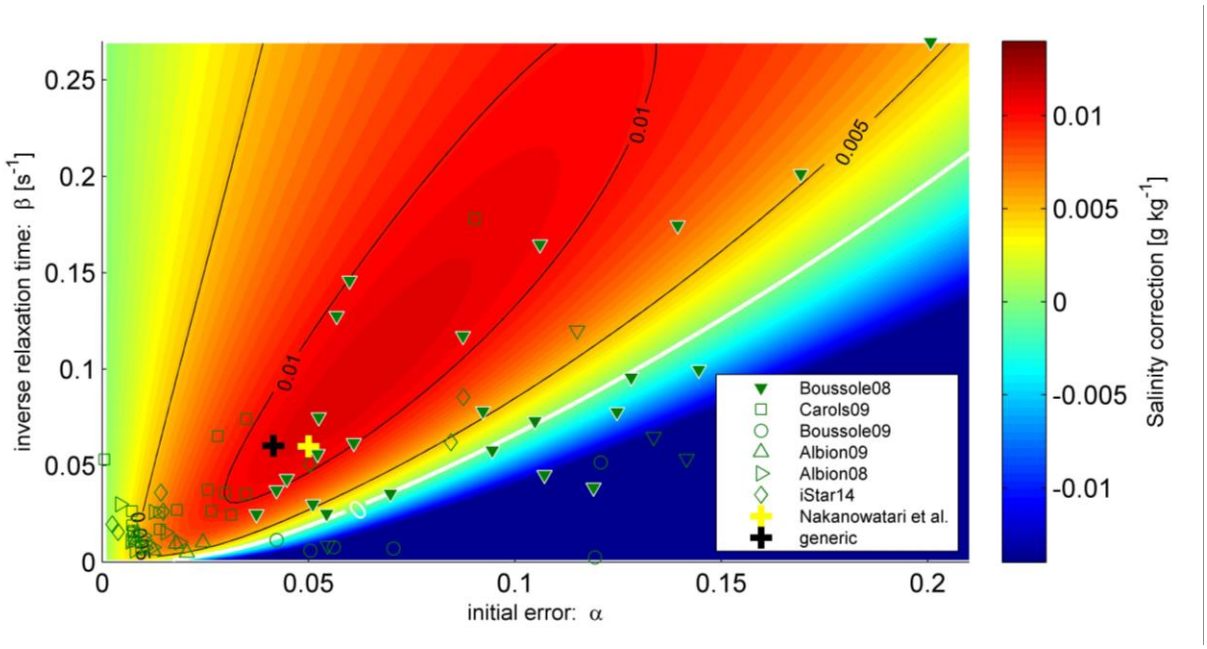

716

717 Figure 6. Salinity correction for different values of coefficients α and β, with $F(\alpha, \beta)$ calculated within ±
718 50 m of the maximum T_{HP} of all the casts tested. The limit of null correction is represented with the white
719 isoline and the various symbols represent the values of optimum coefficients for each profiles for all the
720 experiments tested in this study as well as from the experiment conducted by Nakanowatari et al. (2017).
721 Filled symbols represent those profiles whose maximum T_{HP} exceeds 2.0 °C and empty symbols those
722 whose maximum T_{HP} fall below this limit.

723

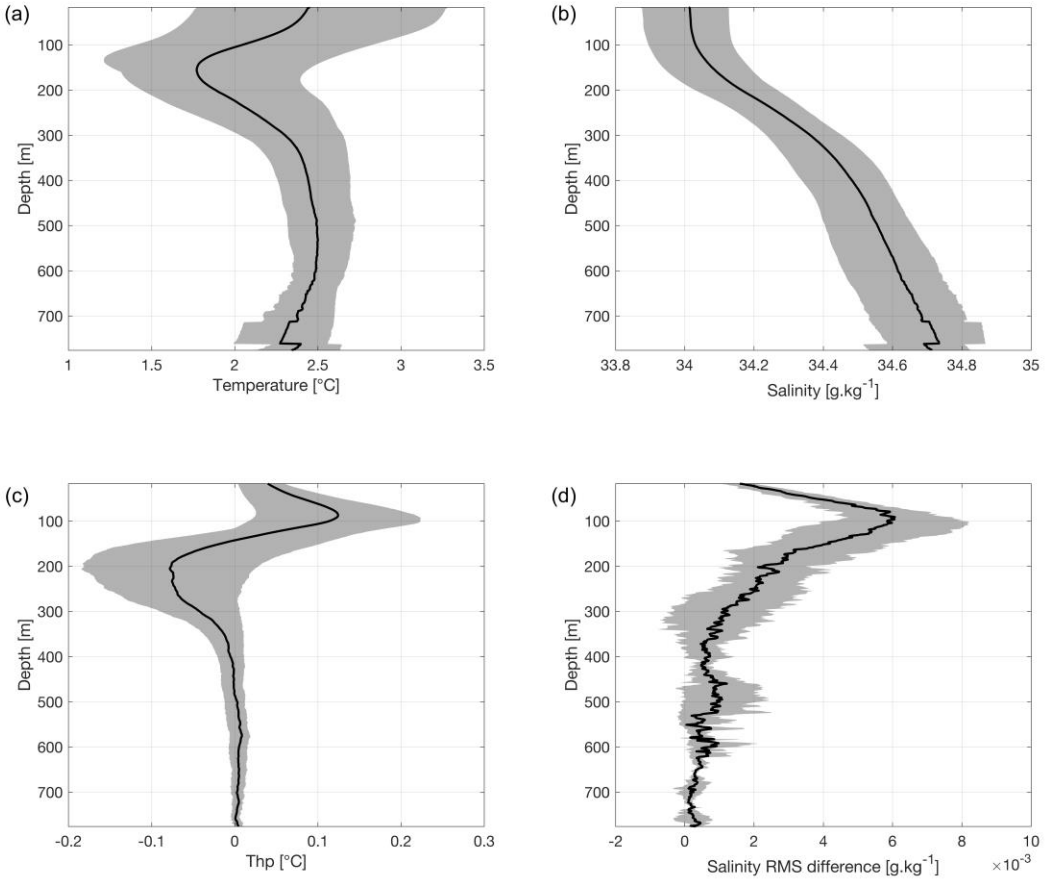

724

725 Figure 7 (a) Mean Temperature, (b) salinity, (c) T_{HP}, (d) RMS_{ad_raw}-RMS_{ad_cor} profiles averaged for all
726 full-resolution CTD-SRDL tags deployed on SES around the Kerguelen Islands. The shaded area
727 envelopes represent the 20th and 80th percentile in all 4 plots.

728

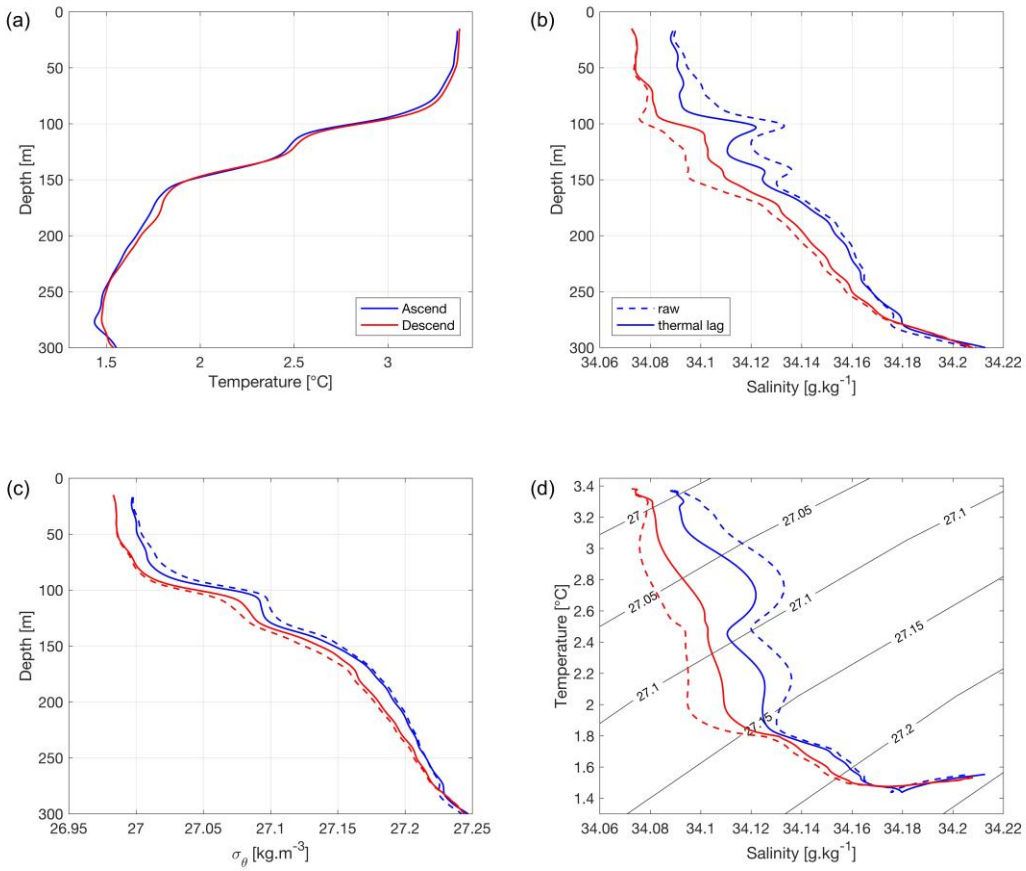

729

730 Figure 8: A typical ascent (blue) and descent (red) profile comparison closed up view on the upper 300 m:
731 (a) Temperature, (b) salinity, (c) potential density, and (d) TS diagram. On panels (a), (b) and (c), dashed
732 lines represent raw profiles and solid lines represent the corrected profiles. To enhance visibility, a
733 gaussian filter with a 5dbar window was applied on the profiles.

734